ARTICLE

3D Road Network Modeling and Road Structure Recognition in Internet of Vehicles

Dun Cao[1], Jia Ru[1], Jian Qin[1], Amr Tolba[2], Jin Wang[1] and Min Zhu[3,*]

[1]College of Computer and Communication Engineering, Changsha University of Science and Technology, Changsha, 410114, China

[2]Department of Computer Science, Community College, King Saud University, Riyadh, 11437, Saudi Arabia

[3]College of Information Science and Technology, Zhejiang Shuren University, Hangzhou, 310015, China

*Corresponding Author: Min Zhu. Email: zhumin@zjsru.edu.cn

ABSTRACT

Internet of Vehicles (IoV) is a new system that enables individual vehicles to connect with nearby vehicles, people, transportation infrastructure, and networks, thereby realizing a more intelligent and efficient transportation system. The movement of vehicles and the three-dimensional (3D) nature of the road network cause the topological structure of IoV to have the high space and time complexity. Network modeling and structure recognition for 3D roads can benefit the description of topological changes for IoV. This paper proposes a 3D general road model based on discrete points of roads obtained from GIS. First, the constraints imposed by 3D roads on moving vehicles are analyzed. Then the effects of road curvature radius (Ra), longitudinal slope (Slo), and length (Len) on speed and acceleration are studied. Finally, a general 3D road network model based on road section features is established. This paper also presents intersection and road section recognition methods based on the structural features of the 3D road network model and the road features. Real GIS data from a specific region of Beijing is adopted to create the simulation scenario, and the simulation results validate the general 3D road network model and the recognition method. Therefore, this work makes contributions to the field of intelligent transportation by providing a comprehensive approach to modeling the 3D road network and its topological changes in achieving efficient traffic flow and improved road safety.

KEYWORDS

Internet of vehicles; road networks; 3D road model; structure recognition; GIS

1 Introduction

Internet of Vehicles (IoV) refers to the connection of vehicles with the internet, creating an interconnected network. This enables communication between vehicles and their surroundings, facilitating information sharing [1,2]. Furthermore, wireless communication between vehicles can be utilized for collaborative and automatic control, reducing traffic congestion, accidents, and energy consumption [3]. IoV provides a new approach to solving traffic problems. However, the data generated by vehicle

requires real-time processing, as vehicle movement is constrained by road space and time [4,5]. Three-dimensional (3D) road network modeling can describe the topology of IoV and predict the location information of vehicles more accurately. Therefore, studying 3D road modeling in IoV can provide more accurate road network topology for vehicles to obtain time-varying relative position information [6] and improve wireless channel estimation [7], resource coordination and optimization [8], as well as provide computationally intensive and delay-sensitive applications for resource-constrained mobile devices in Multi-Access Edge Computing (MEC) to solve multi-data computing [9–11], which is of great practical significance.

Traditional road network research focuses on the typical road network structure, dividing it into geometric and topological structures for evaluation. However, this research lacks comprehensiveness and cannot meet the demands of the intelligent traffic environment [12,13]. Some studies have utilized satellite remote sensing data to establish road extraction models, but image quality and resolution can affect accuracy, and connection between different roads is not considered [14,15]. With the development of artificial intelligence, some literatures are established road network models to predict traffic flow in intersections and other scenarios, but factors such as sampling rate can impact accuracy and reliability [16,17]. Furthermore, some researchers have tested network protocols and algorithms on road models based on real maps, without examining how different road network structures and road features affect [18,19]. Therefore, this paper comprehensively considers road network structure and features to establish a general 3D road network mathematical model. This modeling approach is more realistic and intuitive, providing higher accuracy and reliability for intelligent transportation systems. Additionally, it can offer more precise spatial information for smart city planning and management.

To facilitate the exploration of the constraints imposed on vehicle moving by the structure features of the 3D road network, this paper utilizes available GIS road discrete points to establish a general mathematical model for 3D road network that is suitable for IoV scenarios. Additionally, it designs a regional 3D road network structure recognition and feature extraction algorithm. The main contributions of this paper can be summarized as follows:

- By analyzing how the road structure constrains the vehicle's movement, this paper classifies the 3D road into intersections and road sections. A general mathematical model of the 3D road network is established to provide a theoretical basis for vehicle trajectory prediction in IoV, and four features are defined to depict different 3D road section structures.

- Based on the data obtained from the GIS, this paper analyzes the discrete points of road source data and proposes an intersection node extraction algorithm. The structure and features of the road sections in the region are identified based on the topological relationships between the intersection nodes.

- Finally, this paper uses the real discrete point data of a certain region in Beijing to establish a simulation scenario that evaluates the general 3D road model and the recognition methods of intersection and road section. The experiments verify the effectiveness of the proposed model and methods.

The rest of the paper is organized as follows: Section 2 reviews the related work; Section 3 analyzes how the 3D road constrains the movement of vehicles and establishes a general model of the 3D road network; Section 4 explores the intersection and road section recognition method and road feature extraction method used for the 3D road; Section 5 validates the model and methods; finally, Section 6 provides conclusions.

2 Related Work

Road network modeling forms the basis for the analysis of road networks, mainly including the structure of road networks, road data support, and road network attribute features. In a systematic study of road network structure, Li et al. studied cities with typical road networks, summarized four basic road network forms, and clarified the importance of reasonable urban road network structures in road network planning [20]. To achieve an accurate description of the urban road network shape, Tsiotas et al. divided road network shape characteristics into two categories, namely geometric shape and topological structure, and compared modern urban road networks with computer technologies such as Origin and DepthMap X [21]. Courtat et al. contended that cities should combine topological structures with geometric shapes and introduced geometric graphs and hypergraphs based on simplified streets for road network modeling [22]. Turner recognized that the road centerline can be applied in GIS, a corner segment analysis method is proposed and combined with axial and road centerline representation [23]. Lu et al. proposed a method based on point cloud generate a 3D vulnerable road model with geometric shape and texture information. However, the model does not consider complex road scenes and lacks discussion on the application and impact in the actual traffic safety field [24].

For the support of road data in road networks, the traditional methods of road information extraction can be divided into four categories: GPS trajectory clustering methods, area methods, knowledge models, and artificial mapping methods [25]. Among the commonly used GPS trajectory clustering methods, road networks are mostly obtained by sample sparsity and GPS data center fitting processing. But the road networks generated by this method cannot directly reflect the morphological changes of roads and other features [26]. In recent years, relevant scholars have used deep neural networks to extract high-resolution road information from urban road remote-sensing images. Some scholars used a convolutional neural network (CNN) to classify the pixels of the road image of the input network into road and non-road categories. However, this method was costly and labor-intensive [27]. Wang et al. conducted initial semantic segmentation of images based on road scenes to extract road information [28]. He et al. proposed a loss function-optimized UNet network to completely extract urban roads without object occlusion [29]. The ResNet network simplifies the deep neural network learning framework and can achieve excellent road extraction performance [30,31].

For the research on road network attribute features, Rivera-Royero et al. performed an investigation of connectivity, redundancy, accessibility, reliability, and the other performance indicators used to establish a program that can evaluate the advantages and disadvantages of the road network and draw more attention to reliability [32]. Scott et al. argued that a traffic network should not only satisfy origin-destination requirements, but provide sufficient connectivity to avoid interference with individual road sections within the system [33]. Yin et al. argued that connectivity was not related to the dynamic characteristics of the network, etc., but to its topology [34]. Cheng et al. argued that existing studies did not consider road scenarios and could not effectively solve the connectivity problem in large-scale connectivity problems in heterogeneous vehicular networks, so a connectivity model for vehicular networks in intersection scenarios was developed [35]. Emami et al. comprehensively reviewed the latest developments and characteristics of IoV related technologies. By comparing pilot tests around the world, they found that although there were many research projects in this area, there was a single study and few practical applications [36]. Zheng et al. presented mathematical modeling of lanes and intersections for lane-level road networks for autonomous vehicle driving. Unfortunately, the mathematical model that describes the different type of road sections like straight line and arc curve is ignored during the modeling process [37].

This paper not only focuses on the structure of typical road network, but constructs a general mathematical model for 3D road networks that can be applied to all road structures by incorporating their relevant attributes. In establishing the mathematical model, we have utilized GIS discrete points with higher precision and ease of analysis to fit the road centerline. Moreover, we proposed intersection and road section recognition algorithms as well as road feature extraction algorithms to further enhance the reliability of the model.

3 Modeling

As both communication and data processing nodes, the continuous movement of a vehicle will impact the relative position of the node, thus resulting in dynamic changes to the topology in IoV [38]. A 3D road model is capable of providing a more precise depiction of actual roads compared to a two-dimensional (2D) model, which can more effectively predict vehicle trajectories [39]. Consequently, by analyzing the constraints imposed by the 3D road on vehicle trajectories, we found that the 3D road composed of road sections with different features and the connected intersection structure will constrain the vehicle driving. Then, a general 3D road network model is established for constraining vehicle movements in IoV based on the topological relationship between the intersection and road.

3.1 Analysis of Constraints on Vehicle Movement by 3D Roads

3D road network is an interconnected network composed of intersections and roads between intersections. Since this paper uses the available road discrete points to model the road network, the road is defined as starting from the center point of one intersection to the center point of another intersection, which is composed of sections with similar or identical features. When a vehicle travels as a node in IoV, it may traverse various types of road sections and intersections. A road network region example is presented in Fig. 1. The vehicle V1, V2 and V3 travel on roads A, B, C and D, which are connected by Intersection 1, 2 and Intersection 3. The current positions of the vehicles are P1, P2 and P3, respectively. During the driving process, they will be assisted by the base station and the roadside unit for information interaction. Road A includes a straight section of road, which is called Section 1 and a curved road section is Section 2. Road B and C are straight roads, and Road D is curved road.
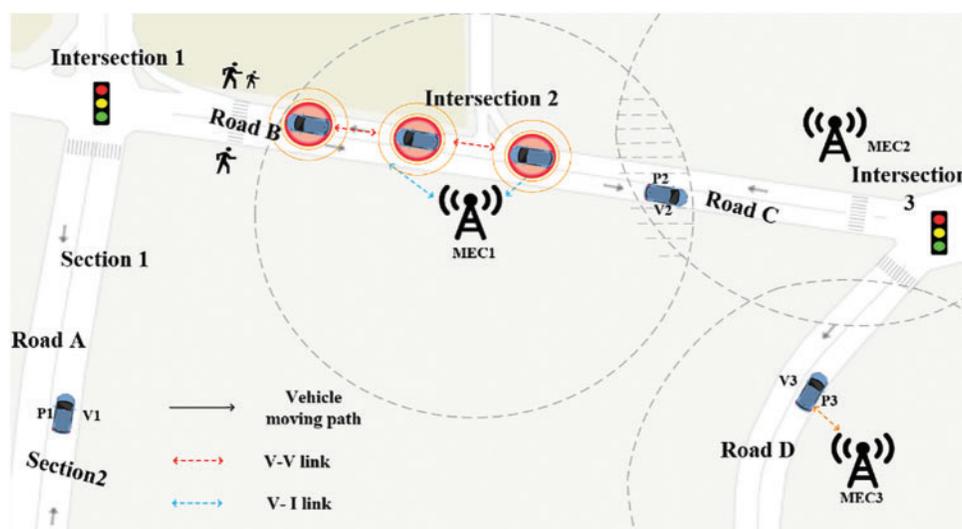

Figure 1: Example of road network region

Suppose that vehicle V1 is currently traveling on the curved Section 2 of Road A with an initial velocity. As V1 continues to move along this section, the curvature and length of Section 2 will impact both the direction and value of the vehicle's acceleration. Upon entering the straight Section 1, V1 will determine its acceleration value based on the length of the upcoming straight road, and its acceleration direction based on the center line of the straight road. Then, when V1 enters the Intersection 1 connected to Section 1, V1 will have three choices: turn left, go straight, or turn right. Consequently, the number and distribution of connected branches will determine the vehicle's trajectory. At this time, the change of acceleration depends not only on the features of the current section, but on the connectivity and topology of the road region in the direction of motion. Furthermore, while driving on 3D roads, such as overpasses, mountain roads, and other scenes, the vehicle will also be influenced by the slope of the road.

Based on the above analysis, different 3D road features will constrain the vehicle's trajectory in different ways by changing the value and direction of the vehicle's acceleration, thereby affecting the relative distance between nodes in IoV. So the main features of the road section are summarized as its radius of curvature, slope, length and starting and ending position. Meanwhile, the features of the intersection are its location information and connected road indicators. A 3D road network can be described as a collection of roads and intersections made up of road sections.

3.2 Model of 3D Road Network

To simplify the 3D road model, the width of the road and the number of lanes is ignored, such that the road network is modeled with the centerline of the road in the data source. The paper establishes a 3D road and intersection model to form a network model through integration.

Each 3D road is composed of all road sections inside the road along with the center points of the intersections that connected with the road. The general model for a 3D road is represented as:

$$Road = f_{Rd} (Roadsection, node), \tag{1}$$

where $Roadsection = \{rodesec_0, \ldots, rodesec_i, \ldots, rodesec_I\}$ $i \in [0, I]$ is the set of all sections of the road, $I + 1$ represents the number of the contained sections, and $node$ is the center point of the intersection connecting the road. It should be noted that the cover of the center point in $Road$ is intended to connect to the intersection. And $f_{Rd}()$ is the function that matches $Roadsection$ and $node$ to $Road$.

Here, the model $rodesec_i$ by mapping the features of position information (Pos), radius of curvature (Ra), longitudinal slope (Slo), and length (Len) to the 3D section model through a function $f_{Rs}()$ is given as:

$$roadsec_i = f_{Rs} (Pos_i, Ra_i, Slo_i, Len_i), \tag{2}$$

We assume that the vehicle is initially located on a certain section $rodesec_i$ with $J + 1$ discrete points and the position of the vehicle is $Pos_m = (x_m, y_m, z_m)$ $m \in [1, J - 1]$, $Pos_{m-1} = (x_{m-1}, y_{m-1}, z_{m-1})$ and $Pos_{m+1} = (x_{m+1}, y_{m+1}, z_{m+1})$ are two adjacent discrete points of Pos_m.

Feature Ra_i of $roadsec_i$ is the average of the radius of curvature values ra_m of every three adjacent discrete points projected onto a 2D plane. Therefore, the curvature radius Ra_i can be expressed as:

$$Ra_i = \frac{1}{J - 1} \sum_{m=1}^{J-1} ra_m, \tag{3}$$

where the ra_m and the center (x_i^m, y_i^m) of the 2D plane can be represented as:

$$ra_m = (x_m - x_i^m)^2 + (y_m - y_i^m)^2, \tag{4}$$

$$x_i^m = \frac{de - bg}{bc - ad}, \tag{5}$$

$$y_i^m = \frac{ag - ce}{bc - ad}, \tag{6}$$

where $a = x_{m-1} - x_m$, $b = y_{m-1} - x_m$, $c = x_{m-1} - x_{m+1}$, $d = y_{m-1} - x_{m+1}$,
$e = \{[(x_{m-1})^2 - (x_m)^2] - [(y_{m-1})^2 - (y_{m-1})^2]\}/2$, $g = \{[(x_{m-1})^2 - (x_{m+1})^2] - [(y_{m+1})^2 - (y_{m-1})^2]\}/2$.

Slo_i is the average of the longitudinal slope values between every two adjacent discrete points. When $x_m = x_{m+1}$ or $\frac{y_m - y_{m-1}}{x_m - x_{m-1}} = \frac{y_{m+1} - y_m}{x_{m+1} - x_m}$, the section is a straight section and its Ra does not exist; thus, the above equation is not needed for calculation. The method for calculating the Slo_i of $roadsec_i$ is given as:

$$Slo_i = \frac{1}{J+1} \sum_{m=0}^{J} slo_m, \tag{7}$$

where $slo_m = \dfrac{z_{m+1} - z_m}{\left\| (x_{m+1} - x_m)^2 + (y_{m+1} - y_m)^2 \right\|_2}$.

Len_i is the sum of the Euclidean distances between every two adjacent discrete points. Specially, the Euclidean distance between two discrete points is calculated as:

$$EM_{Pos_i}^{Pos_j} = \left\| (x_j - x_i)^2 + (y_j - y_i)^2 + (z_j - z_i)^2 \right\|_2. \tag{8}$$

The calculation for the length value Len_i of $rodesec_i$ be expressed as:

$$Len_i = \frac{1}{J+1} \sum_{m=0}^{J} len_m, \tag{9}$$

where $len_m = EM_{Pos_m}^{Pos_{m+1}}$.

The model of intersections with K ($K \geq 3$) branches can be expressed as:

$$Intersection = f_{Is}(roadsec_1, \dots, roadsec_k \dots, roadsec_K, node), K \geq 3, \tag{10}$$

where $roadsec_k$ is the k-th branch of the intersection, $node$ represents the central node of the intersection, and $f_{Is}()$ is the match relationship.

3D general road network model can be expressed as:

$$RNmodel = f_{Rm}(Road, Node, Intersecion), \tag{11}$$

Notably, the function $f_{Rm}()$ combines the models of *Intersection* an *Road* with the intersection center node set $Node = \{node_0, \dots, node_c, \dots, node_C\}, c \in [0, C]$. $C + 1$ indicates that the contained intersection central nodes.

4 Methods

Previously, the paper analyzed how 3D roads constrain vehicle motion in IoV and summarized the features of roads and intersections. Additionally, a mathematical model of 3D road networks was established by utilizing the topological association between roads and intersections. To establish the corresponding model of each region, this section further uses the relationship between discrete points to propose an intersection recognition algorithm and a road section recognition algorithm. Furthermore, a structural feature extraction algorithm is proposed for various sections and intersections to facilitate a more comprehensive description of the modeling of 3D road networks in different regions.

4.1 Analysis of Source Data

In IoV, vehicles can acquire 3D discrete point data of surrounding roads from GIS. The 3D discrete points possess longitude, latitude, and elevation properties, represented as x, y, and z. By utilizing the 3D information of the data points, the Euclidean distance between two points can be determined, and a sequence of adjacent points, consisting of the nearest points, can be established. Adjacent point groups are made up of two continuous adjacent points. On the road section, there is a tiny phase difference between adjacent point groups. However, because there are several branches of roads, there may be a huge phase difference between adjacent point groups in a crowded region. To create a 3D road network that incorporates both the intersection model and the 3D road model in the vehicle driving region, this paper then uses the difference of vector angles to recognize the intersection and the road section, then uses the road topology to extract the road structural features.

4.2 Intersection Recognition Algorithm

In IoV, vehicles act as information sources or task-initiating nodes, which need to acquire information about the roads within a certain region to infer the future change of the network topology. Assume that at any time t, the current location of the vehicle is denoted as Pos_0, while the set of discrete road points within the driving region centered at Pos_0 and with a radius of r is denoted as $D_{r,pos_o} = \{Pos_0, \ldots, Pos_i, \ldots, Pos_R\}$, $i \in [0, R]$. Here, the initial value of r is denoted as r_0, Pos_i represents the i-th 3D discrete point in D_{r,pos_o}. To judge which point is the center of the intersection, the observation range radius r should be smaller than the width of the road lane d and be greater than the average Euclidean distance between the successive road discrete points, i.e., $\frac{1}{R+1}\sum_{i=0,j=i+1}^{i=R-1} EM_{Pos_i}^{Pos_j} \le r \le$ d. When r is not appropriate to make D_{r,pos_o} empty, we increase r by Δr in turn, and the value of Δr is half of r each time until D_{r,pos_o} is not empty. The direction angle difference $\theta (Pos_0, Pos_i)$ is defined as the value of the angle between the vector formed by Pos_0 and any point Pos_i in set D_{r,pos_o} projected onto the horizontal direction and the x-axis of the Cartesian coordinate system. The minimum threshold value for $\theta (Pos_0, Pos_i)$ is given as δ. And the existence of an intersection center point within the road region is determined by comparing δ with $\theta (Pos_0, Pos_i)$. If an intersection center point is found, it is stored in the intersection center point set $Node$. By traversing the source data and using the above algorithm, it is possible to find all intersections in the region. The algorithm is obtained by continuously outputting the intersection nodes. The average time complexity of the algorithm is n ^{2}. The specific implementation steps are presented in Algorithm 1.

Algorithm 1: Intersection recognition algorithm based on Euclidean distance and vector angle

---

Input: vehicle location Pos_0, initial radius r_0, discrete point dataset D_{r,pos_o}, δ, Δr
Output: intersection center point set $Node$.
Begin $Node = \varnothing$, $D_{r,pos_o} = \varnothing$;
    Find the set of discrete points adjacent with point Pos_0 as the center r_0 as the radius D_{r,pos_o};
    if $\left(D_{r,pos_o} == \varnothing\right)$ **then**
        $r = r_0 + \Delta r$;
    end if
    while $\left(D_{r,pos_o} \ne \varnothing\right)$ **do**
        Find the nearest point Pos_d in $D_{p_0,r}$ from Pos_0;
        Calculate the directional angle difference $\theta_0 = \theta (Pos_0, Pos_d)$;
        Find the set of discrete points D_{r,pos_d} in the direction of travel with point Pos_d as the center and r as the radius;
            if $\left(D_{r,Pos_d} == \varnothing\right)$ **then**

(Continued)

Algorithm 1 (continued)

$\qquad\qquad\qquad r = r + \Delta r;$

$\qquad\qquad$ **end if**

$\qquad\qquad$ **while** $\left(D_{r,Pos_d} \neq \varnothing\right)$ **do**

$\qquad\qquad\qquad$ Find the direction vector angle $\theta_i = \theta(Pos_d, Pos_i), Pos_i \in D_{r,Pos_d};$

$\qquad\qquad\qquad$ **if** $(\forall Pos_i, |\theta_i - \theta_0| \leq \delta)$ **then**

$\qquad\qquad\qquad\qquad$ Find the nearest Pos_i points $Pos_{min};$

$\qquad\qquad\qquad\qquad Pos_d = Pos_i, \theta_0 = \theta_{min}(Pos_d, Pos_{min})$

$\qquad\qquad\qquad$ **else if** $(Node == p)$ **then**

$\qquad\qquad\qquad\qquad$ **while** $Node \neq \varnothing$

$\qquad\qquad\qquad\qquad\qquad$ Return $Node$

$\qquad\qquad\qquad\qquad$ **end while**

$\qquad\qquad\qquad$ **end if**

$\qquad\qquad$ **end while**

$\qquad$ **end while**

End

4.3 Road Section Recognition Algorithm

In the current region, after using Algorithm 1 to recognize intersections, the boundary points set $Lim = \{lim_0, \ldots, lim_m, \ldots, lim_M\}, m \in [0, M]$ and all discrete points set $D = \{Pos_0, \ldots, Pos_u, \ldots, Pos_U\}$, $u \in [0, U]$ of the road network can be obtained, along with the set $Node$ obtained by Algorithm 1. The Euclidean distance and vector angle relationship between discrete points can be further utilized to recognize the road sections from the road. We propose Algorithm 2 to traverse the region from the boundary point and sequentially stores the obtained section discrete points in set $Roadsection$ and remove from Lim. When the traversal encounters an intersection node, it is stored in the set $Roadsection$ and the current section is ended, but not removed the intersection node. If it encounters a boundary point, the search for the current section end and is removed. This process is repeated until the set Lim are traversed. Assuming that there are other discrete points in set D besides intersection nodes, we think that there are sections between intersections that have not been recognized. Then, our algorithm selects the nearest intersection center point of any discrete point except the intersection node, defines it as a new initial boundary point to traverse the section in set D until all the remaining discrete point sets are intersection points. Through the above algorithm, all road sections in the region can be recognized and stored in set $Roadsection$. The algorithm finds the Pos_{nd} according to the basic operation and calculates the average time complexity $\log^2 n$. The specific implementation steps are shown in Algorithm 2.

Algorithm 2: Road section recognition algorithm

Input: road boundary point set Lim, road discrete point set D, and intersection node set $Node$.

Output: road section set $Roadsection$.

Begin

$\qquad$ **Initialization:** $i = 0, \forall i \in [0, I], m = 0, \forall m \in [0, M], Pos_{start} = Lim_0;$

$\qquad$ **while** $(D \neq Node)$ **do**

$\qquad\qquad$ Delete Pos_{start} from $Lim;$

$\qquad\qquad$ Delete Pos_{start} from $D;$

$\qquad\qquad$ Find Pos_{start} adjacent point Pos_{next} with Euclidean distance, $Pos_{start} = Pos_{next};$

$\qquad\qquad roadsec_i[0] = roadsec_i \cup \{Pos_{start}\};$

$\qquad\qquad$ **while** $(Lim \neq \varnothing)$ **do**

Algorithm 2 (continued)

       if ($Pos_{start} \notin Lim$ **or** $Pos_{start} \notin Node$) **then**

          $roadsec_i = roadsec_i \cup \{Pos_{start}\}$;

          Delete Pos_{start} from D;

          Find Pos_{start} adjacent point Pos_{next}, $Pos_{start} = Pos_{next}$;

          if ($Pos_{start} \in Node$) **then**

             $roadsec_{i++}[0] = roadsec_i \cup \{Pos_{start}\}$;

          else if ($Pos_{start} \in Lim$)**then**

             Delete Pos_{start} from Lim;

             Delete Pos_{start} from D;

             $Pos_{start} = Lim_{++m}$;

             $roadsec_{i++}[0] = roadsec_i \cup \{Pos_{start}\}$;

          end if

       end if

     end while

     if ($D \neq Node$) **then**

       for $s = 0, 1, \ldots, \text{len}(D) - 1$, $Pos_{start} = D_{s++}$ **do**

         if ($Pos_{start} \notin Node$) **then**

          Find Pos_{start} near intersection node Pos_{nd} by Algorithm1;

          $Pos_{start} = Pos_{nd}$;

          $Lim_m = Pos_{start}$;

         end if

       end for

     end if

   end while

  Return *Roadsection*;

End

4.4 Road Structural Feature Extraction Algorithm

In the previous, recognition of intersection and road sections was completed. Then we introduce Algorithm 3 to match additional sections according to the position of the intersection center point. This method achieves structural recognition of intersection branches in different regions. The mathematical model of intersections and road sections described in Section 3.2 is used to extract the curvature radius, longitudinal slope, length, and position features of the section and the specific structure and features of the road network are obtained. In this paper, we define the road sections that are connected to the current vehicle to be stored in the connected set *Conroadsec* = {}. By matching the vehicle position with the road section set *Roadsection*, the current road section of the vehicle can be recorded as $roadsec_0$. The average time complexity n of the algorithm is obtained by calculating the output of the algorithm. Specific implementation as Algorithm 3, while Fig. 2 displays the flow chart of road structure feature extraction.

Algorithm 3: Road structure feature extraction algorithm

Input: road section set *Roadsection*, $roadsec_0$.

Output: connected set *Conroadsec*, *Ra*, *Slo*, *Len*.

Begin

   Initialization: *Conroadsec* = $\varnothing$, *Ra* = $\varnothing$, *Slo* = $\varnothing$, *Len* = $\varnothing$;

(Continued)

Algorithm 3 (continued)

    for (i = 1 to N) **do**

        if ($roadsec_i \cap roadsec_0 \cap Node \neq \varnothing$) **then**

            $Conroadsec_i = rodesec_i$;

        end if

    end for

    for (i = 0 to N) **do**

        Calculate ra of the $roadsec_i$ by using Eqs. (3)–(5);

        if $\left(\dfrac{y_m - y_{m-1}}{x_m - x_{m-1}} = \dfrac{y_{m+1} - y_m}{x_{m+1} - x_m} \quad \text{or} \ (x_m = x_{m-1} \text{ and } x_m = x_{m+1}) \right)$ **then**

            $rodesec_i[1] = 0$;

        else

            $rodesec_i[1] = ra$;

        Calculate slo of the $roadsec_i$ by using Eq. (7);

            $rodesec_i[2] = slo$;

        Calculate len of the $roadsec_i$ by using Eq. (9);

            $rodesec_i[3] = len$;

    end for

  Return $Conroadsec$, Ra, Slo, Len

End
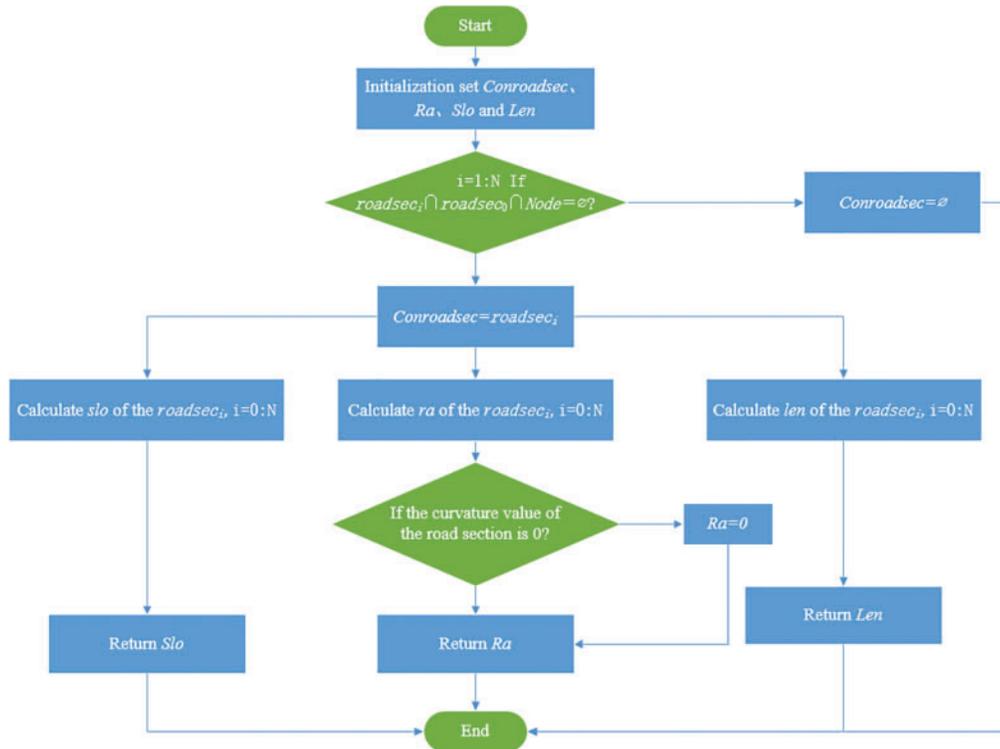
Figure 2: Flowchart of road structure feature extraction algorithm

5 Discussions on Experimental Results

This section simulates the real road region to verify the general model of 3D road network and the proposed algorithm. The measured indicators include the compatibility of the intersection region with the region's intersection region, the model whether can recognize the structure of the region's road, and the connectivity between the roads. The simulation results compared with real maps data demonstrates excellent performance.

5.1 Simulation Setup

The 2D GIS data from the main roads in Beijing's Fourth Ring Road were used in this paper and obtained from OpenStreetMap (OSM). The 2D geographic data of road network was separated with the ArcMap software package, while the generation of the road centerlines was processed with the sampling tool Arc Toolbox. The reasonable engineering specifications and constraints were adopted to extend 2D discrete points to 3D road data for the simulation environment. For demonstration, two complex overpass regions, Wanghe Overpass and Siyuan Overpass, as well as the main road of East North Fourth Ring Road connecting the two overpass regions, are selected for the subsequent simulation. The geographical region extends from longitude 116°25′16″ to 116°29′52″ and latitude 39°57′43″ to 39°59′40″, and was processed by the 3D road network platform as the testing region.

5.2 Verification of Intersection and Road Section Recognition

To verify the effectiveness of Intersection and Road Section Recognition Algorithms, three locations were selected as the vehicle's position in the 3D map. As Fig. 3 shows, the geographical coordinates of the vehicle are as follows: Location A (116.452153, 39.977029, 0); Location B (116.436289, 39.986742, 0); and Location C (116.462122, 39.970931, 4.5).

Figure 3: Simulation region with selected location

The experimental of this paper considers the constraints of the communication range of vehicles in IoV, and uses a circular region with r of 50 m to recognize intersections and road sections. In the Locations A, B and C, we recognized the roads in the region of Location A between Beijing Wanghe

Overpass and Siyuan Overpass, Location B of Wanghe Overpass and Location C of Siyuan Overpass, which compared them with the actual road structure, respectively, as shown in Figs. 4–6. At Location A, our model successfully recognized three roads. At Location B, our model can accurately identify five roads and one intersection. However, the road on the left side of Section 5 looks close in the 2D plane, but beyond the 3D spherical area is not recognized. At Location C, our model successfully identified two intersections and seven roads, including sections of the overpass. The experimental results of this paper show that the proposed 3D road and intersection recognition model has high accuracy and reliability, and can accurately identify the road structure in different regions. In the future, it can be effectively applied to traffic management and real-time traffic monitoring in vehicle communication range.
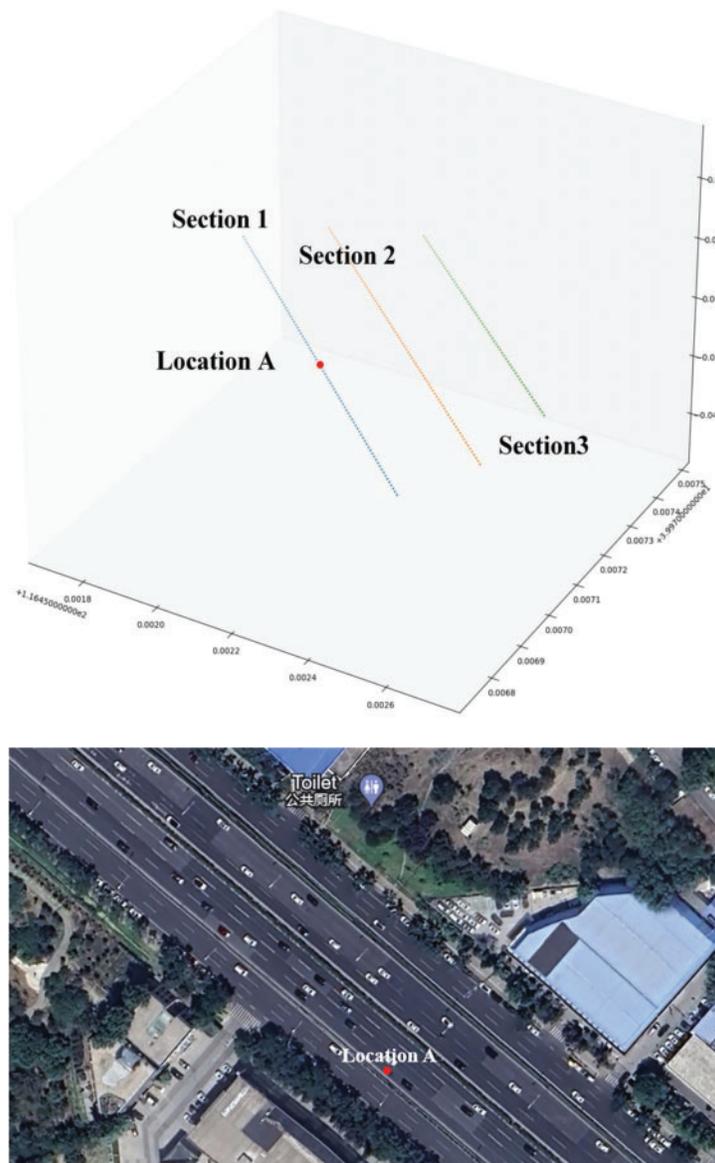

**Figure 4:** Road section recognition and map comparison-Location A
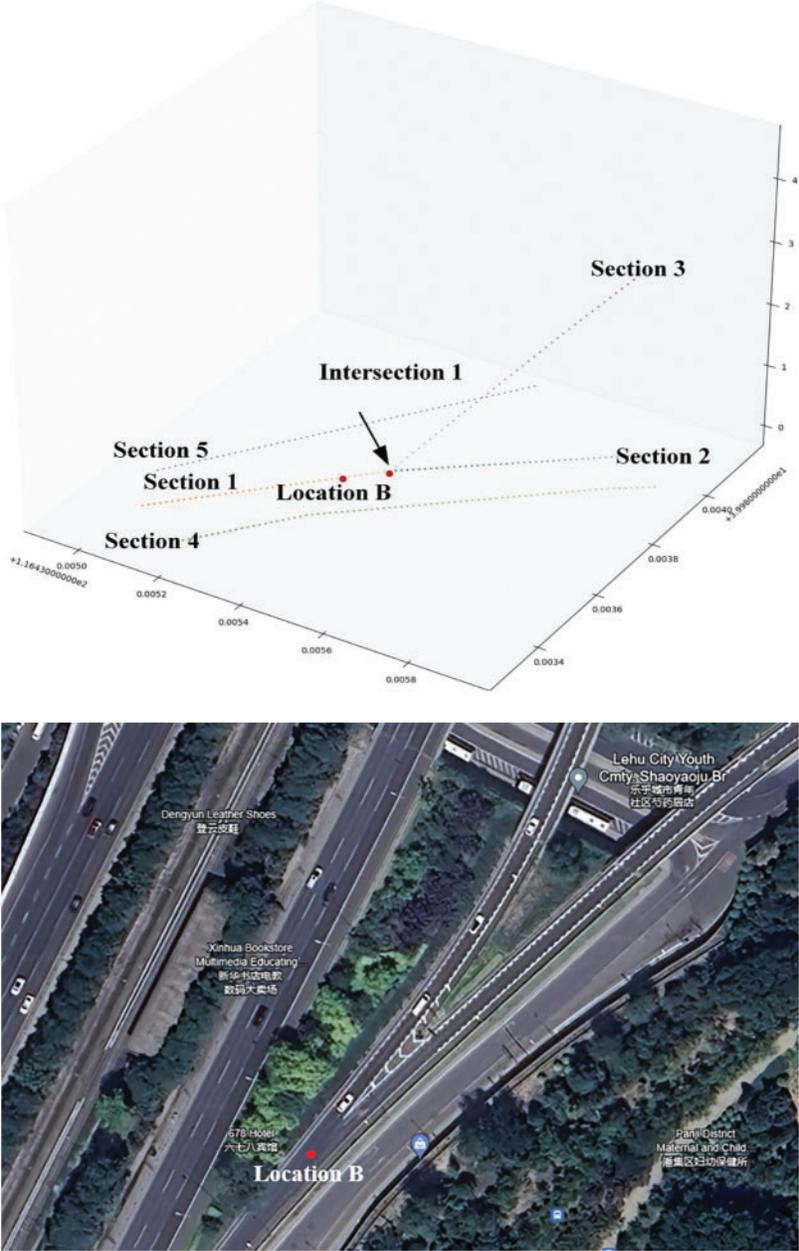
Figure 5: Road section and intersection recognition and map comparison-Location B
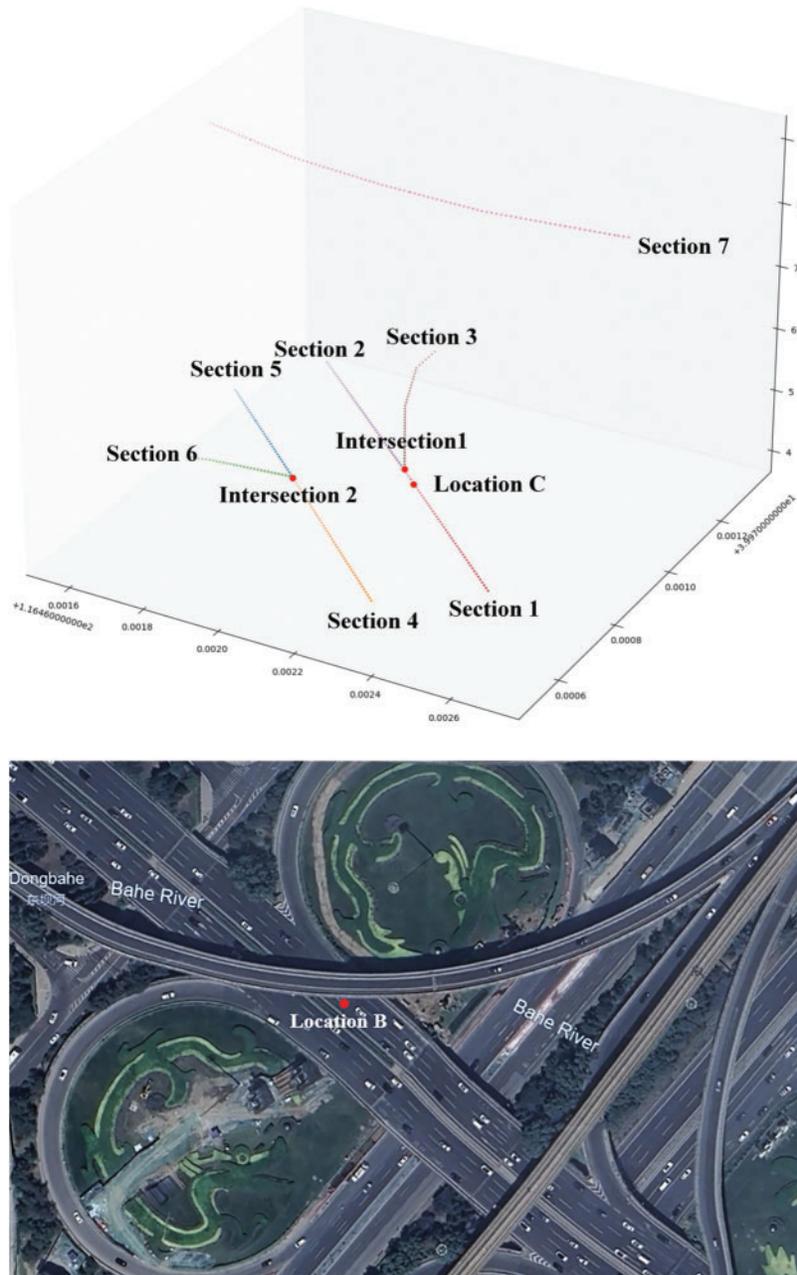
Figure 6: Road section and intersection recognition and map comparison-Location C

5.3 Verification of Road Structural Feature Extraction

The extraction results for the three regions in terms of road structure feature with Algorithm 3 are presented in Tables 1–3. The output results include the following: the latitude, longitude, and elevation of the location, as well as the intersection center point; whether the intersection or section is connected to the road section; and the curvature radius (m), longitudinal

slope (%), length (m), and lowest point elevation (m) of the road section. A feature that does not exist is denoted by "−". For example, Curvature Radius does not exist when the road section is straight.

Table 1: Road structural feature extraction results-vehicle position A

Location	Intersection nodes	Connectivity	Section number	Connectivity	Curvature radius	Slope	Length	L-point elevation
(116.452153, 39.977029, 0)	—	—	1	Not connected	—	2.3	98.48	0
			2	Not connected	—	2.3	91.69	0
			3	Not connected	—	2.3	70.49	0

Table 2: Road structural feature extraction results-Location B

Location	Intersection nodes	Connectivity	Section number	Connectivity	Curvature radius	Slope	Length	L-point elevation
(116.45215, 39.977029, 0)	(116.435415, 39.983709, 0)	Connections	1	Connections	—	1.2	49.01	0
			2	Connections	—	1.3	49.63	0
			3	Connections	—	5.5	49.67	0
			4	Not connected	343.06	1.2	93.38	0
			5	Not connected	—	1.2	94.02	0

Table 3: Road structural feature extraction results-Location C

Location	Intersection nodes	Connectivity	Section number	Connectivity	Curvature radius	Slope	Length	L-point elevation
(116.462122, 39.970931, 4.5)	(116.461913, 39.970815, 4.5)	Connections	1	Connections	—	4.3	49.94	4.5
			2	Connections	—	4.3	49.15	4.5
			3	Connections	100.09	4.1	50.70	4.5
	(116.462122, 39.970931,4.5)	Connections	4	Not connected	—	4.3	50.43	4.5
			5	Not connected	—	4.3	39.10	4.5
			6	Not connected	—	4.1	31.28	4.01
		Not connected	7	Not connected	232.03	1.4	99.63	9.0

Table 1 shows the road structural feature extraction results in the region of Location A. The results explain that there is no intersection node and no road connectivity in this region. The longitudinal slopes of Sections 1, 2 and 3 are 2.3%; The longitudinal slopes of all road sections are all 2.3%. Section 1 is 98.48 m in length, Section 2 is 91.68 m, Section 3 is 70.49 m. The lowest elevation of all three road sections in this region is 0. The road features extracted from the Location A region are compared on the map, showing that the features extracted in this paper have an error of less than 1 m, and the results are accurate.

The road structural feature extraction results in Table 2 are for Location B in the region. The results show that there is one intersection node at the geographical coordinate of (116.435415, 39.983709, 0), which connects Sections 1, 2, and 3. Sections 1, 2, 3, and 5 are all straight, while Section 4 has a curvature radius of 343.06 m. The slope of Section 1 is 1.2%, Section 2 is 1.3%, Section 3 is 5.5%, Section 4 is 1.2%, and Section 5 is 1.3%. Moreover, the length of Section 1 is 49.01 m, Section 2 is 49.63 m, Section 3 is 49.67 m, Section 4 is 93.38 m, and Section 5 is 83.67 m. The lowest elevation

for all road sections is 0. The road features extracted from the Location B region were meticulously compared on the map, demonstrating that the feature length extracted in this paper has negligible error of less than 0.5 m, an impressively low curvature of less than 1 m and a slope of just 0.01. This indicates that the model is exceptionally reliable.

Table 3 shows the road structural feature extraction output results in the region of Location C, which contains two intersection nodes, and the geographical coordinates are (116.461913, 39.970815, 4.5) and (116.462122, 39.970931, 4.5), respectively. The intersection 1 is connected to the Sections 1, 2 and 3. Intersection 2 connects Sections 4, 5, and 6, but there is no connectivity between intersections 1 and 2. Except for Sections 3 and 7, all road sections are straight. The curvature radius of Section 3 is 100.09 m, and Section 7 is 232.03 m. The slope of the Section 1, Section 2, Section 4, and Section 5 is all 4.3%, Section 3 and Section 6 are 4.1%, and Section 7 is 1.4%. The length of Section 1 to Section 7 is 49.94, 49.15, 50.7, 50.7, 39.10, 31.28, and 99.63 m. The lowest elevations of Sections 1, 2, 3, 4, and 5 are all 4.5 m, but the lowest elevation of Section 6 is 4.01 m, and the lowest elevation of Section 7 is 9 m. The road features extracted from the location C region are compared with the distance on the map, which proves that the feature error extracted in this paper is within a reasonable range and can be used for subsequent research.

5.4 Verification of 3D Road Network

To illustrate the establishment of the 3D road network model, this paper selects a representative overpass as an example due to the presence of elevation differences in space and complex road structures. The simulation verification is carried out in the Wanghe Overpass where vehicle B is located. Algorithms 1 and 2 are utilized to identify intersections and roads in the selected region, while Algorithm 3 extracts structural features of road sections. Fig. 7 illustrates the recognized road network structure.
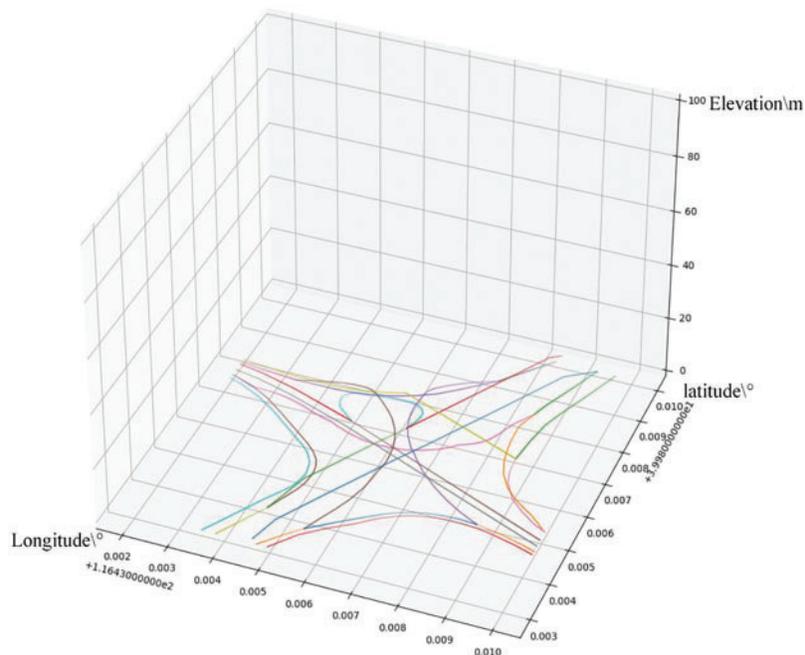

Figure 7: Verification of 3D road network—Wanghe overpass

To assess the accuracy of the simulation results, Fig. 8 displays the matching degree of the recognized road network against the real image of the overpass, using different colors to distinguish various roads. The comparison reveals that the simulation results effectively capture the road type features like straight roads, curves, and ramps in the overpass region, thus demonstrating the efficacy of the road network model proposed in this study.
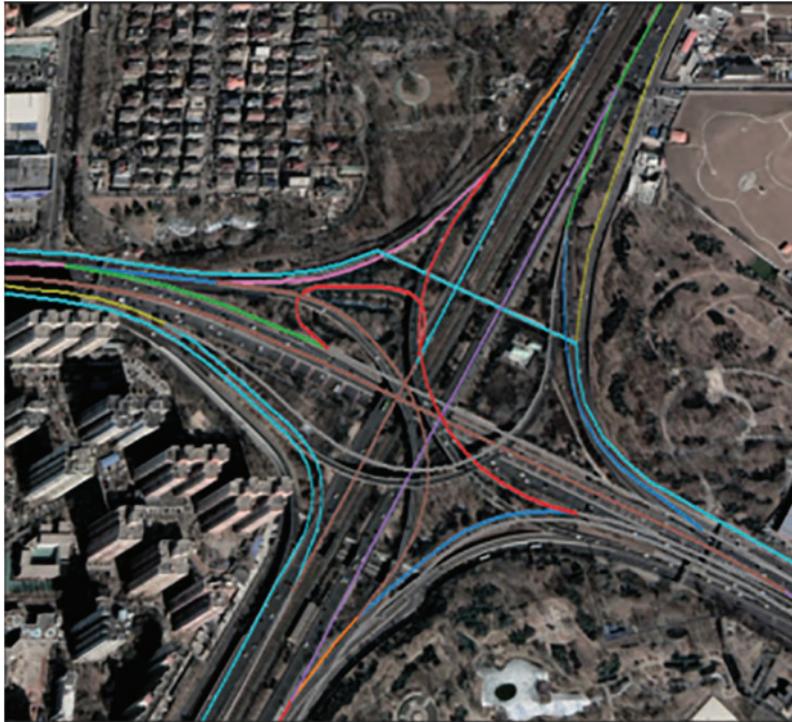

Figure 8: Comparison diagram of Wanghe overpass and simulation model

6 Conclusions and Future Works

In this paper, a general 3D road network mathematical model based on discrete points by GIS is proposed, which can extract road features and recognize road structures. To extract the essential features of roads, the paper has analyzed their impact on vehicle travel and created road network models that comprise a 3D road section model and an intersection model. A road structure featured extraction algorithm is proposed that leverages vector angles and Euclidean distances between 3D discrete points to identify intersections and road sections. It is promising to realize vehicle trajectory prediction and relay node selection within the constraints of the road network in IoV, thereby providing more accurate and comprehensive information on traffic flow, congestion, and accessibility in different regions, and providing more accurate map data for intelligent transportation systems such as autonomous driving. However, the current research strategy has some limitations. Firstly, this paper simplifies the constraint of road structure on vehicle driving to a linear structure of road centerline without considering multi-lane models or road width. Secondly, even though this paper considers objective factors that restrict vehicle driving, the limitations on vehicle driving conditions also include subjective characteristics.

In future work, we aim to improve the algorithm, consider additional road features and structures, and establish an even more intelligent road network model.

Author Contributions: The authors confirm contribution to the paper as follows: study conception and design: D. C., J. R., M. Z.; data collection: J. Q., A. T.; analysis and interpretation of results: D. C., J. R., J. Q.; draft manuscript preparation: J. R., J. Q., J. W. All authors reviewed the results and approved the final version of the manuscript.

Availability of Data and Materials: The data involved in this study are all public data, which can be downloaded through public channels.

Conflicts of Interest: The authors declare that they have no conflicts of interest to report regarding the present study.

References

1. Xu, Z., Liang, W., Li, K. C., Xu, J., Jin, H. (2021). A blockchain-based roadside unit-assisted authentication and key agreement protocol for internet of vehicles. *Journal of Parallel and Distributed Computing, 149,* 29–39.

2. Gerla, M., Lee, E. K., Pau, G., Lee, U. (2014). Internet of vehicles: From intelligent grid to autonomous cars and vehicular clouds. *Proceedings of 2014 IEEE World Forum on Internet of Things (WF-IoT)*, pp. 241–246. Seoul, Korea (South).

3. Zhang, D., Li, G., Zheng, K., Ming, X., Pan, Z. H. (2014). An energy-balanced routing method based on forward-aware factor for wireless sensor networks. *IEEE Transactions on Industrial Informatics, 10(1),* 766–773.

4. Wang, J., Han, H., Li, H., He, S., Sharma, P. K. et al. (2021). Multiple strategies differential privacy on sparse tensor factorization for network traffic analysis in 5G. *IEEE Transactions on Industrial Informatics, 18(3),* 1939–1948.

5. He, S., Xie, K., Xie, K., Xu, C., Wang, J. (2019). Interference-aware multisource transmission in multiradio and multichannel wireless network. *IEEE Systems Journal, 13(3),* 2507–2518.

6. Cai, X., Liu, K., Hu, Z., Zhang, Y. (2021). An algorithm for constructing road network using block polygon topology. *Geomatics and Information Science of Wuhan University, 46(8),* 1170–1177.

7. Tang, Q., Yu, Z., Jin, C., Wang, J., Liao, Z. et al. (2022). Completed tasks number maximization in UAV-assisted mobile relay communication system. *Computer Communications, 187,* 20–34.

8. Cao, D., Zeng, K., Wang, J., Sharma, P. K., Ma, X. et al. (2021). BERT-Based deep spatial-temporal network for taxi demand prediction. *IEEE Transactions on Intelligent Transportation Systems, 23(7),* 9442–9454.

9. Zhang, D., Wang, W., Zhang, J., Zhang, T., Du, J. et al. (2023). Novel edge caching approach based on multi-agent deep reinforcement learning for internet of vehicles. *IEEE Transactions on Intelligent Transportation Systems, 24(6),* 1–16.

10. Deo, N., Trivedi, M. M. (2018). Convolutional social pooling for vehicle trajectory prediction. *Proceedings of the Conference on Computer Vision and Pattern Recognition*, pp. 1468–1476. Salt Lake City, UT, USA.

11. Zhou, S., Netalkar, P. P., Chang, Y., Xu, Y., Chao, J. (2018). The MEC-based architecture design for low-latency and fast hand-off vehicular networking. *Proceedings of the 2018 IEEE 88th Vehicular Technology Conference (VTC-Fall)*, pp. 1–7. Chicago, IL, USA.

12. Tuohy, S., Glavin, M., Hughes, C., Jones, E., Trivedi, M. et al. (2014). Intra-vehicle networks: A review. *IEEE Transactions on Intelligent Transportation Systems, 16(2),* 534–545.

13. Perera, S., Perera, H. N., Perera, K. (2018). Topological structure of the road traffic network in the western regional Megapolis, Sri Lanka. *Proceedings of the 2018 Moratuwa Engineering Research Conference (MERCon)*, pp. 37–42. Moratuwa, Sri Lanka.

14. Wan, J., Xie, Z., Xu, Y., Chen, S., Qiu, Q. (2021). DA-RoadNet: A dual-attention network for road extraction from high resolution satellite imagery. *IEEE Journal of Selected Topics in Applied Earth Observations and Remote Sensing, 14,* 6302–6315.

15. Tao, M., Ding, Z., Cao, Y. (2021). Attention U-Net for road extraction in remote sensing images. *SpatialDI 2020: Spatial Data and Intelligence*, pp. 153–164.

16. Li, L., Jiang, R., He, Z., Chen, X. M., Zhou, X. (2020). Trajectory data-based traffic flow studies: A revisit. *Transportation Research Part C: Emerging Technologies, 114,* 225–240.

17. Olayode, I. O., Tartibu, L. K., Okwu, M. O. (2021). Prediction and modeling of traffic flow of human-driven vehicles at a signalized road intersection using artificial neural network model: A South African road transportation system scenario. *Transportation Engineering, 6,* 100095.

18. Yusuf, T. A., Altilar, D. T. (2017). Impact on inter-vehicular communication performance on different traffic mobility model: A case study of ad hoc on-demand distance vector routing protocol. *Proceedings of the International Conference on Computing for Engineering and Sciences*, pp. 6–12. New York, NY, USA.

19. Peng, W., Dong, G., Yang, K., Su, J. (2013). A random road network model and its effects on topological characteristics of mobile delay-tolerant networks. *IEEE Transactions on Mobile Computing, 13(12),* 2706–2718.

20. Li, D., Shi, Z., Li, D., Dong, P., Xing, J. (2018). The analysis and optimization of urban transit network based on complex networks. *Proceedings of the 2018 IEEE 4th Information Technology and Mechatronics Engineering Conference (ITOEC)*, pp. 1154–1158. Chongqing, China.

21. Tsiotas, D., Polyzos, S. (2017). The topology of urban road networks and its role to urban mobility. *Transportation Research Procedia, 24,* 482–490.

22. Courtat, T., Gloaguen, C., Douady, S. (2011). Mathematics and morphogenetics of cities: A geometrical approach. *Physical Review, 83(3),* 36106.

23. Turner, A. (2007). From axial to road-centre lines: A new representation for space syntax and a new model of route choice for transport network analysis. *Environment and Planning B: Planning and Design, 34(3),* 539–555.

24. Lu, W., Zhao, D., Premebida, C., Zhang, L., Zhao, W. et al. (2023). Improving 3D vulnerable road user detection with point augmentation. *IEEE Transactions on Intelligent Vehicles, 8(5),* 3489–3505.

25. Gu, Q., Xue, B., Song, J., Li, X., Wang, Q. (2022). A high-precision road network construction method based on deep learning for unmanned vehicle in open pit. *Mining, Metallurgy & Exploration, 39(2),* 397–411.

26. Zhang, J., Hu, Q., Li, J., Ai, M. (2020). Learning from GPS trajectories of floating car for CNN-based urban road extraction with high-resolution satellite imagery. *IEEE Transactions on Geoscience and Remote Sensing, 59(3),* 1836–1847.

27. Li, P., Zang, Y., Wang, C., Li, J., Cheng, M. et al. (2016). Road network extraction via deep learning and line integral convolution. *Proceedings of the 2016 IEEE International Geoscience and Remote Sensing Symposium (IGARSS)*, pp. 1599–1602. Beijing, China.

28. Wang, Q., Gao, J., Yuan, Y. (2017). Embedding structured contour and location prior in siamesed fully convolutional networks for road detection. *IEEE Transactions on Intelligent Transportation Systems, 19(1),* 230–241.

29. He, H., Wang, S., Wang, S., Yang, D., Liu, X. (2019). A road extraction method for remote sensing image based on encoder-decoder network. *Acta Geodaetica et Cartographica Sinica, 48(3),* 330−338.

30. Zhang, L. (2021). Vehicle-road collaborative recognition method based on ResNet and improved SSD. *Proceedings of the 2021 IEEE 2nd International Conference on Big Data, Artificial Intelligence and Internet of Things Engineering (ICBAIE)*, pp. 527–530. Nanchang, China.

31. Cao, D., Dai, R., Wang, J., Ji, B., Alfarraj, O. et al. (2023). Fast visual tracking with squeeze and excitation region proposal network. *Human-Centric Computing and Information Sciences, 13,* 1–20.

32. Rivera-Royero, D., Galindo, G., Jaller, M., Reyes, J. B. (2022). Road network performance: A review on relevant concepts. *Computers & Industrial Engineering, 165,* 107927.

33. Scott, D. M., Novak, D. C., Aultman-Hall, L., Guo, F. (2006). Network robustness index: A new method for identifying critical links and evaluating the performance of transportation networks. *Journal of Transport Geography, 14(3),* 215–227.

34. Yin, H. Y., Xu, L. Q. (2010). Measuring the structural vulnerability of road network: A network efficiency perspective. *Journal of Shanghai Jiaotong University (Science), 15,* 736–742.

35. Cheng, J., Mi, H., Huang, Z., Gao, S., Zang, D. et al. (2017). Connectivity modeling and analysis for internet of vehicles in urban road scene. *IEEE Access, 6,* 2692–2702.

36. Emami, A., Sarvi, M., Asadi Bagloee, S. (2022). A review of the critical elements and development of real-world connected vehicle testbeds around the world. *Transportation Letters, 14(1),* 49–74.

37. Zheng, L., Li, B., Yang, B., Song, H., Lu, Z. (2019). Lane-level road network generation techniques for lane-level maps of autonomous vehicles: A survey. *Sustainability, 11(16),* 4511.

38. He, S., Li, Z., Wang, J., Xiong, N. N. (2020). Intelligent detection for key performance indicators in industrial-based cyber-physical systems. *IEEE Transactions on Industrial Informatics, 17(8),* 5799–5809.

39. Al-Obaidi, A. S., Jubair, M. A., Aziz, I. A., Ahmad, M. R., Mostafa, S. A. et al. (2022). Cauchy density-based algorithm for VANETs clustering in 3D road environments. *IEEE Access, 10,* 76376–76385.